Scientia Iranica D (2023) 30(2), 577–591

SCIENTIA IRANICA

Sharif University of Technology
Scientia Iranica
Transactions D: Computer Science & Engineering and Electrical Engineering
http://scientiairanica.sharif.edu

Separation of the fetal heart signal in a synchronous network consisting of maternal and fetal hearts

N. Zandi-Mehran and S.M.R. Hashemi Golpayegani*

Department of Biomedical Engineering, Amirkabir University of Technology, Tehran 15875-4413, Iran.

Received 15 January 2021; received in revised form 28 May 2021; accepted 23 August 2021

KEYWORDS
Fetal monitoring;
Non-invasive;
Feto-maternal monitoring;
Networks;
Synchronization;
Chaos;
Signal separation.

Abstract. This paper studies the heart oscillation model to separate fetal ECG from maternal ECG based on abdominal recordings. To this end, two phases are designed. A modified version of the Duffing-Van der Pol oscillator is considered a computational heart model at the modeling phase. To evaluate the effect of the interaction between maternal and fetal hearts as well as the differences and features of the fetal heart structure, the fetal heart model is modified based on the maternal heart model. A non-identical network is employed as an interactive network of the maternal and fetal hearts. Then, the degree of network synchronization is measured using a pattern synchronization index of the non-identical network. An attempt is made to separate the fetal signal from the maternal signal in abdominal signals at the separation phase. Two problem-solving approaches are explained: the step-by-step mode that calculates the signal at any given moment and the construction of general equations. These approaches are used to calculate the variables, including maternal and fetal signals, making it possible to separate the maternal ECG from fetal one.

1. Introduction

Cardiovascular problem is one of the most common congenital diseases that remains undiagnosed even years after birth [1]. Therefore, recording fetal cardiac activities monitors fetal heart performance. The results show that fetal electrocardiogram (fECG) can identify most disorders in the hearts of mother and fetus [2]. In addition, the prominence of fECG over Cardiotocography (CTG) in the fetal heart disease diagnosis was reported in [3,4]. Since most fetal diseases can be detected possibly by studying fECG, a complete analysis of fECG signal can prevent such drawbacks [5]. However, recording fECG signals contains is not without critical challenges [6,7].

The fECG signal can be obtained via direct or indirect procedures [6]. The direct method is invasively using wire electrodes on the fetus scalp or abdomen [8]. Due to the dangers of the direct method, a non-invasive procedure was utilized in [9,10]. In such methods, ECG signals are recorded over the mother's abdomenal surface. The recorded signal is the abdominal ECG (aECG), which consists of fetal and maternal electrocardiograms (mECG). Given that the mECG amplitude is significantly larger than the fECG amplitude, recovery of fECG from aECG is quite challenging [11]. Consequently, many studies have investigated different separation methods to fulfill the aim [5,12].

*. *Corresponding author. Tel.: +98 21 64542370*
E-mail addresses: nazaninznd@yahoo.com (N. Zandi-Mehran); mrhashemigolpayegani@aut.ac.ir (S.M.R. Hashemi Golpayegani)

doi: 10.24200/sci.2021.57540.5292

Several methods including adaptive filtering method [13–15], genetic algorithm [16], Singular Value Decomposition (SVD) [11,17], Independent Component Analysis (ICA) [18–21], and wavelet transform analysis [22,23] have been employed in order to extract the fECG signal from the aECG. Adaptive filters are divided into two groups: stochastic gradient approach and recursive least square algorithms [24]. In these algorithms, the crucial issue is to set correct parameters [25]. The SVD technique reduces noise and separates components [11] within the constraint on the number of recording electrodes, which must be more than sources [26]. ICA is a Blind Source Separation (BSS)-based method that is used when sources are independent [27]. The method presented in [28] functions based on the FastICA algorithm. Wavelet transform is another technique used for time-scale domain analysis [29]. In [22], Datian and Xuemei detected the mECG signal edges using spline wavelet transform and then, extracted the mECG signal by finding the local maximum of aECG. In addition to the mentioned approaches, such methods as artificial intelligence [30], maternal ECG pattern [31], Gaussian moments [32], time structure information, and high-order statistical components related to fetal ECG signal [33] are utilized to extract fECG from aECG signal. Here, the computational model is introduced as an approach to fECG extraction.

Computational modeling provides the best mathematical representation of a system [34]. The computational biological models provide a virtual laboratory that characterizes the complex system features [35]. An appropriate theoretical model mainly highlights essential features and underplays insignificant details of the natural system [36]; thus, such a model can be the right approach to illustrating heart activities. The heart is a complex, adaptable system that operates effectively due to the interactions of its dynamic parts [37]. Former studies have found the ECG signal to be periodic [36]. However, the heart as a biological system shows evolutionary properties [38]. On this matter, the authors in [39] stated that the hierarchical model was a viable way to simulate the properties of such a complex system since agents are the main components of this model.

Chaos has been investigated in various biological systems as a long-term non-periodic behavior in a deterministic system, sensitive to the initial conditions [40,41]. The unpredictability of the complex behavior of chaotic systems is one of the crucial factors in modeling biological systems with complex features [42]. The cardiovascular system as a biological system can be considered a chaotic system [43–45]. In [46], the positive Lyapunov exponents of the RR-interval signal were extracted from the pulse signal of finger capillaries, which pointed out that the heart had a chaotic behavior. Chaos in cardiac myocytes has also been shown in many experimental studies and modeling. For instance, Chialvo et al. indicated that the cardiac Purkinje fibers could bifurcate due to their chaotic dynamics [47].

Many studies have investigated the heart at microscopic, mesoscopic, and macroscopic levels [48]. In this study, macroscopic models have been proposed for the heart dynamical function based on Van der Pol oscillators [49]. Some modified Van der Pol models have been introduced by incorporating physiological features of the heart dynamics [50,51]. In another study, the coefficients of a modified Van der Pol oscillator as a computational model of the heart were optimized using neural network algorithms [52]. In [53], two Van der Pol oscillators were coupled as a cardiac model in which one of the oscillators was assumed to represent the dynamics of the heart pacemaker. Some research used a three-coupled Van der Pol oscillator (SA node, AV node, and HP complex) to discuss the heart rhythm implementation and model it in a macroscopic state [54,55]. To investigate the dynamics of the mother and fetus hearts, the interaction should consider a network.

From a systemic perspective, a network consists of nodes and their connections that can sometimes create the most crucial form of dynamical collective behavior, i.e., synchronization [56,57]. Each node demonstrates a dynamical system in such networks, and their connections represent the interaction between them. Networks of identical oscillators with the same parameter values, called identical lattices, can produce complete synchronization [58]. However, non-identical networks can never be fully in synch [59,60]. Real-world systems, such as biological and engineering networks, are non-identical [61]. In 2020, Panahi and Jafari proposed an approximate synchronization index [62], inspired by the Poincaré section. Unlike conventional methods, this method provides a quantitative index for measuring the degree of behavioral synchronization, focusing on the pattern of fluctuations in the network.

This paper is organized as follows: In Section 2, a heart model is presented and also, the maternal and fetal heart interaction is modeled. In Section 3, the synchronization of this network is investigated. Besides, the system equations are generated through time variation in this section. In Section 4, the approach to separating fetal signals from the abdominal signal is introduced. Finally, in Sections 5 and 6, the discussion and conclusions are presented, respectively.

2. Model

2.1. The heart model

Nonlinear oscillators are used as computational models to show the normal or abnormal heart rhythm. In this study, a nonlinear Modified Duffing-Van der Pol

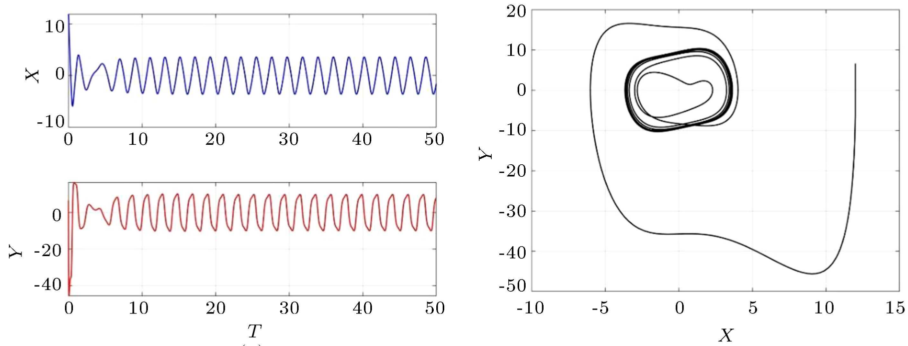

Figure 1. (a) The time series and (b) phase space of Duffing-Van der Pol model with respect to parameters $a = 0.2$, $b = 5.8$, and $c = 3$ corresponding to the initial condition $(12, 6.6)$.

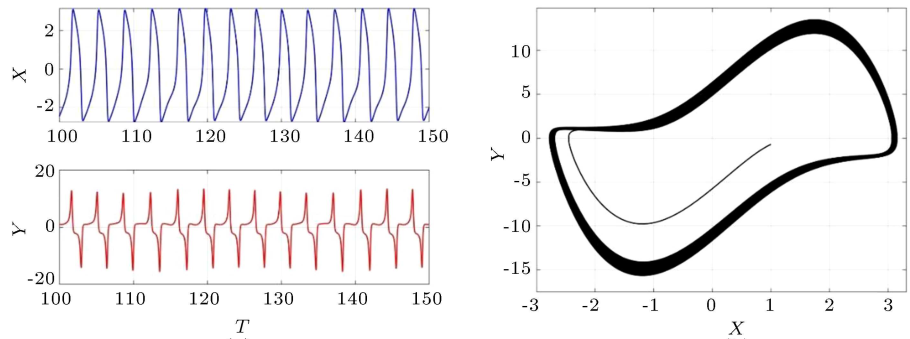

Figure 2. (a) The time series and (b) phase space of modified Duffing-Van der Pol model with respect to parameters $a = 2.5$, $b = 1.8$, $c = 3.8$, $w_1 = 1.8$, and $w_2 = 1.2$ with initial condition $(1, -0.7)$.

oscillator is proposed as a computational model of the heart rhythm. Since heart rhythms have been claimed to be chaotic signals [43,44], many researchers have attempted to reconstruct the heart signal model based on the chaotic oscillator. The Modified Van der Pol oscillator has drawn wide attention among different oscillator models as it can achieve different aspects of the heart signal [63]. As an effective parameter, time delay was incorporated into the Van der Pol oscillator as well; thus, it could illustrate the heart oscillation perfectly [51].

Van der Pol equation is a proper choice for modeling heart dynamics systems such as cardiac cycles and heart rate variations. It can also show the heart's relaxation oscillations [50,52]. The qualities of Van der Pol signals are very similar to the heart action potential characteristics. Both slow and fast types of action potentials can be easily simulated using Duffing-Van der Pol. The driving term in each oscillator is responsible for the external input, which is included in Eq. (1). Figure 1 shows the time series and phase space of the Duffing-Van der Pol model in the determined parameters.

$$\ddot{x} - a(1 - x^2)\dot{x} + x^3 = b\cos(ct). \tag{1}$$

The parameters of the Modified Duffing-Van der Pol model are adjusted based on the actual heart signal. It can be formulated as Eq. (2):

$$\begin{cases} \dot{x} = y \\ \dot{y} = -a(x - w_1)(x + w_2)y - x^3 + b\cos(ct). \end{cases} \tag{2}$$

Figure 2 shows the time series and phase space of the heart model using Eq. (2). It indicates the heart chaotic function when the parameters are set to $a = 2.5$, $b = 1.8$, $c = 3.8$, $w_1 = 1.8$, and $w_2 = 1.2$ upon choosing $(1, -0.7)$ as the initial conditions.

The bifurcation diagram is another way of analyzing the chaotic behavior of this model. Hence, the system dynamics are analyzed via the bifurcation diagram concerning the variation of parameter a. In Figure 3, the system bifurcation diagrams are plotted for both x and y variables with two different approaches. In the first approach, the bifurcation diagram is plotted using peaks of the time series (see Figure 3(a) and Figure 3(b)). In the second approach, Inter Spike Intervals (ISI) of the time series are used for plotting the bifurcation diagram in Figure 3(c) and (d). Plotting bifurcation diagrams using max values of the variables shows their amplitude variations. However, plotting ISI bifurcation diagrams reveals the variation in the timing of interspike. Therefore, these bifurcations present two different features of the system dynamics.

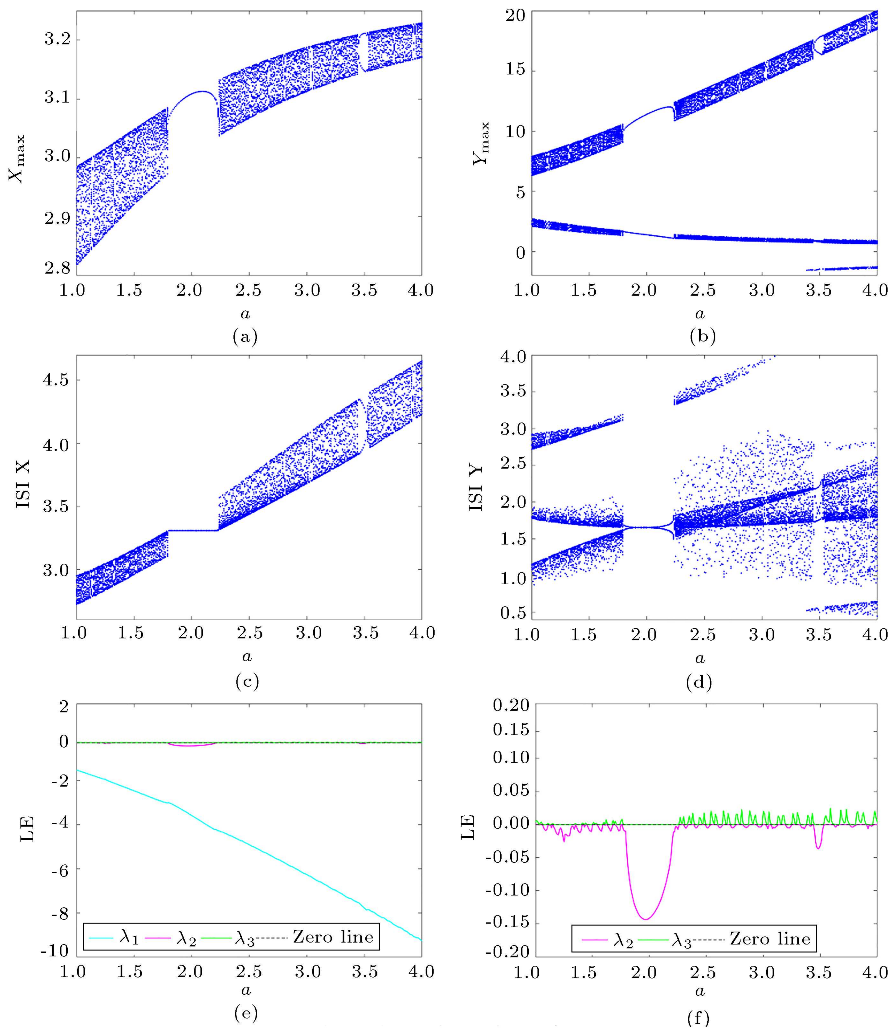

Figure 3. Bifurcation diagrams of the modified Duffing-Van der Pol model using constant initial conditions $[1, -0.7]$. Peak values with changing a as the bifurcation parameter in (a) x variable and (b) y variable. ISIs versus a for (c) x variable and (d) y variable. (e) The corresponding Lyapunov exponent of the Modified Duffing-Van der Pol model, and (f) zoom of the region within $[-0.2, 0.2]$. Other parameters are $b = 1.8$, $c = 3.8$, $w_1 = 1.8$, and $w_2 = 1.2$.

For example, by changing the parameter a in the range of [1.79,2.23], the spike amplitude varies, although the ISI bifurcation shows that the intervals of these spikes are constant. Moreover, a positive Lyapunov exponent is employed to show chaotic dynamics in the system [64]. In Figure 3, below the bifurcation diagrams, the corresponding Lyapunov exponents are plotted via parameter a. As shown in Figure 3(e) and (f), one of the Lyapunov exponents turns positive in the chaotic region.

Complex dynamics can be seen in the model bifurcation diagram according to changes in the other parameters of the model. Figure 4 shows different bifurcation patterns by changing parameters b, c, w_1, and w_2.

2.2. *Fetal heart model*

The amplitude of the fetal ECG is 20% smaller than that of the maternal ECG. In addition, the amplitude value of the cardiac signals in adults is about a few millivolts. Consequently, the fetal signal is much weaker than the maternal one. One of the problems in the mother-fetus signal separation is the constant presence of maternal ECG signal, which is about 5 to 20 times larger than the fetal ECG signal [11]. Therefore, the fetal heart is modeled using a Modified Duffing-Van der Pol, which fluctuates with the intensity of one-twentieth adult heart. To this end, the modified Duffing-Van der Pol concerning the fetus heart model is formulated with scaled variables ($\dot{x} = A\dot{X}$ and $\dot{y} = A\dot{Y}$) as follows:

$$\begin{cases} \dot{x}_2 = \left(\frac{1}{A}\right)(By_2) \\ \dot{y}_2 = \left(\frac{1}{B}\right)\Big(-a(Ax_2 - w_1)(Ax_2 + w_2)y \\ \qquad\qquad -(Ax_2)^3 + b\cos(ct)\Big) \end{cases} \tag{3}$$

To demonstrate how the amplitudes of mECG and

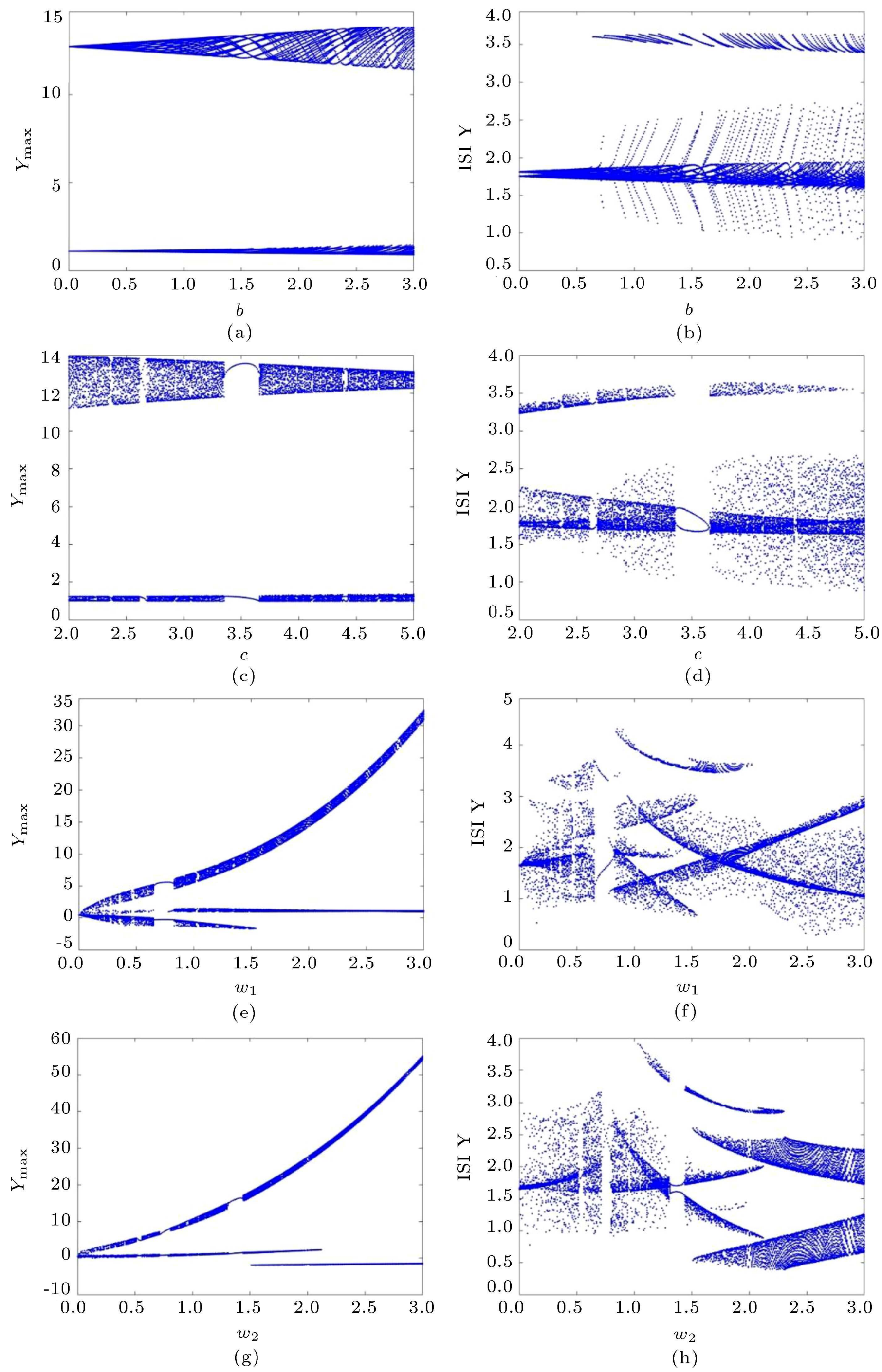

Figure 4. Bifurcation diagrams of the modified Duffing-Van der Pol model for constant initial conditions $[1, -0.7]$: (a) Peak values of y variable and (b) ISIs of y versus b. (c) Peak values and (d) ISIs of y with changing c. (e) Maximum values of y and (f) ISIs of y variable concerning the variation of parameter w_1. (g) Peak values of y variable and (h) ISIs of y versus w_2.

fECG are differentiated in the worst cases, two coefficients A and B are set to 20. The result is plotted in Figure 5.

As shown in Figure 5, coefficients A and B only affect the amplitude intensity; thus, similar results have been obtained concerning the performance and pattern of the two models.

2.3. The interacting network of maternal and fetal hearts

A dynamical network is considered here to investigate the dynamic interaction between the maternal and fetal hearts. The interaction between maternal and fetal hearts is modeled through linear coupling of x

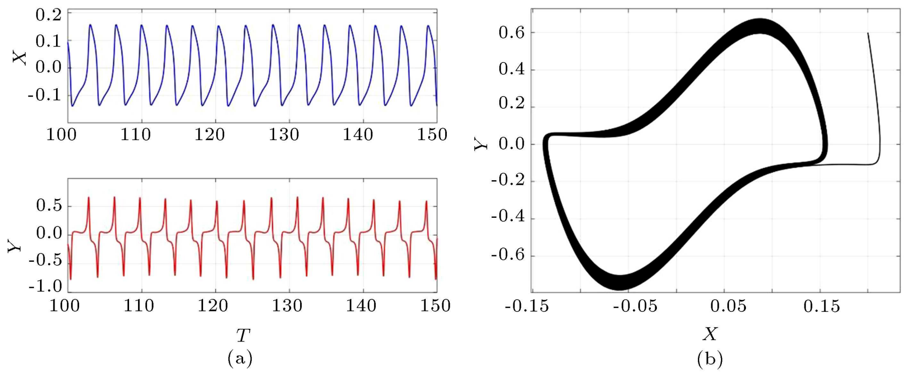

Figure 5. (a) The time series and (b) phase space of Eq. (3) for parameters $A = 20$, $B = 20$, $a = 2.5$, $b = 1.8$, $c = 3.8$, $w_1 = 1.8$, and $w_2 = 1.2$ with initial condition $(0.2, 0.6)$.

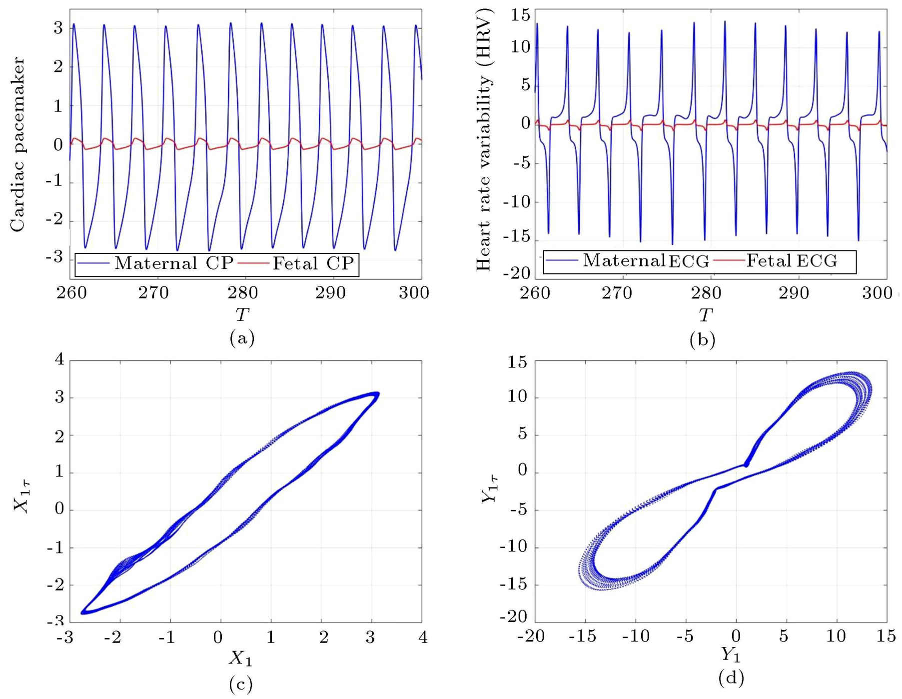

Figure 6. (a) The time series of x variable in fetal in red and maternal in blue, and (b) the time series of y variable in fetal in red and maternal in blue. (c) Delayed phase space of maternal x variable and (d) delayed phase space of maternal variable in Eq. (4) for setting parameters as parameters $A = 20$, $B = 20$, $a = 2.5$, $b = 1.8$, $c = 3.8$, $w_1 = 1.8$, $w_2 = 1.2$, and $\tau = 20$ with initial condition $(1, -0.7, 0.02, 1)$.

variables, which can be formulated as Eq. (4):

$$\begin{cases} \dot{x}_1 = y_1 + \varepsilon(x_2 - x_1) \\ \dot{y}_1 = -a(x_1 - w_1)(x_1 + w_2)y_1 - x_1^3 + b\cos(ct) \\ \dot{x}_2 = \left(\frac{1}{A}\right)(By_2) + \varepsilon(x_1 - x_2) \\ \dot{y}_2 = \left(\frac{1}{B}\right)\Big(-a(Ax_2 - w_1)(Ax_2 + w_2)y_2 \\ \qquad -(Ax_2)^3 + b\cos(ct)\Big) \end{cases} \tag{4}$$

In Eq. (4), ε shows the interaction coefficient (coupling strength), the variable x acts as a Cardiac Pacemaker (CP) in each of the maternal and fetal heart models, and the variable y shows the Heart Rate Variable (HRV). The model outputs are shown in Figure 6 after setting the interaction coefficient to $\varepsilon = 0.01$. Sometimes, chaotic behaviors appear to be irregular and random in time series, but have a strong underlying order in phase space [65]. A phase space projection shows the dependency of each state on the next one; hence, the phase space is used to study chaotic dynamics [66] and topological characteristics of the system [67]. Numerical processes, i.e., estimating the correlation dimension and the Lyapunov exponents or modeling and forecasting the time series, are performed based on phase space [68]. In Figure 6(c) and (d), trajectories pass close together in the delayed phase space.

3. Analysis of synchronization in a non-identical network

From a systemic perspective, a network consists of nodes and their connections that can sometimes create the most crucial form of dynamical collective behavior, i.e., synchronization [56,57]. Each node demonstrates a dynamical system in such networks, and their connections represent the interaction between them. Synchronization is one of the most exciting consequences of interaction in dynamic networks [69]. Networks of identical oscillators with the same parameter values, called identical lattices, can produce complete synchronization [58]. However, non-identical networks can never be fully in synch [59,60]. Real-world systems such as biological and engineering networks are non-identical [61].

Non-identical networks can be divided into two general groups: (1) the same dynamical system with different parameters and (2) different dynamical systems placed at each node [70]. Most of the real-world research studies have investigated non-identical networks of the first group [71]. In 2008, Hill et al. presented conditions for global synchronization for the first group of the non-identical network [72]. Also, other studies were conducted to generalize the existing methods for measuring synchronizes in these networks [73,74]. Then, the approximate synchronization method was considered for both groups of non-identical networks [75]. Approximate synchronization uses measuring similarity in different behavior aspects [76]. A new method (pattern synchronous) based on the behavioral pattern of the network oscillators was proposed to measure synchronization in non-identical complex biological systems [62]. Inspired by the Poincaré section, this method considers inconsistency between the network oscillations as a principle and ignores such parameters as amplitude and phase similarity.

In this method, each time series peak is considered as a sign of complete oscillation. The algorithm of this method begins with finding the peaks of each oscillator of the network. Then, the peaks of different time series are compared and the close peaks are counted, considering the threshold value. Finally, the synchronization degree is then defined, proportional to the number of corresponding peaks in the time series of the network oscillators. In this paper, the synchronous study was carried out using this method since non-identical oscillators interacted. The results are shown in Figure 7.

As illustrated in Figure 7, by enlarging the coupling coefficient, the degree of synchronization increased by calculating and averaging it with 20 random initial conditions to reduce dependence on the initial condition. It can be seen that for coupling strengths larger than 0.01, the two oscillators share the same pattern. Thus, the coefficient of 0.01 is chosen and considered as the coupling coefficient for the rest of this study.

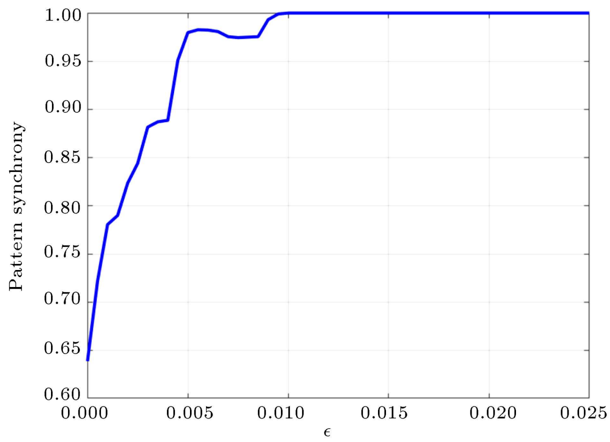

Figure 7. Measuring pattern synchronization index in the coupled maternal and fetal heart model in the different coupling coefficients (ε).

4. Separation

In general, there are two methods for extracting the fECG signal: direct method (invasive) and indirect method (non-invasive). The indirect fECG signal extraction holds significant advantages over other methods. However, this method is subject to some limitations.

As shown in Figure 8, a combination of the maternal and fetal heart signals can be captured with abdominal recording. Therefore, a combined signal of the maternal and fetal hearts, i.e., $y_1 + y_2$, is recorded.

In the following, we are looking for a way to separate the fetal signal from the collective signal $y_1 + y_2$. A fragment of this signal is shown in Figure 9.

Suppose that the heart's systemic model and

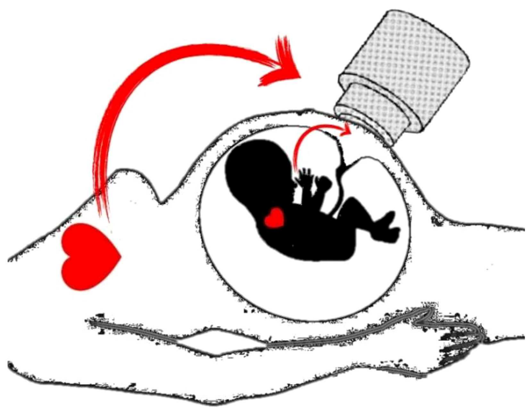

Figure 8. Combination of the maternal and fetal heart signals in abdominal recording. Higher intensity of the maternal heart signal than that of fetal heart signal was shown with a thicker arrow.

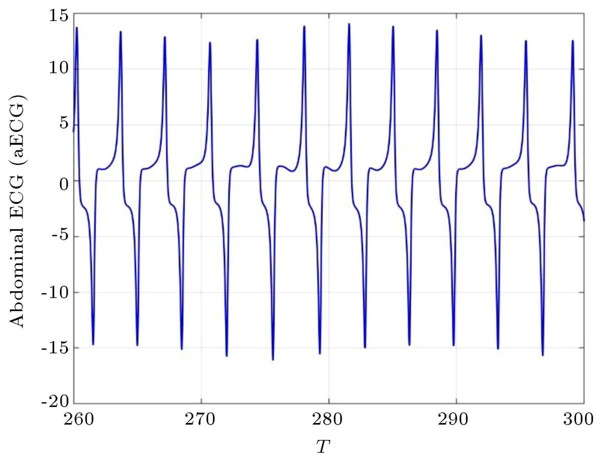

Figure 9. Assuming abdominal recording, time series of the combined heart signal of the mother and the fetus, $y_1 + y_2$, from Eq. (4).

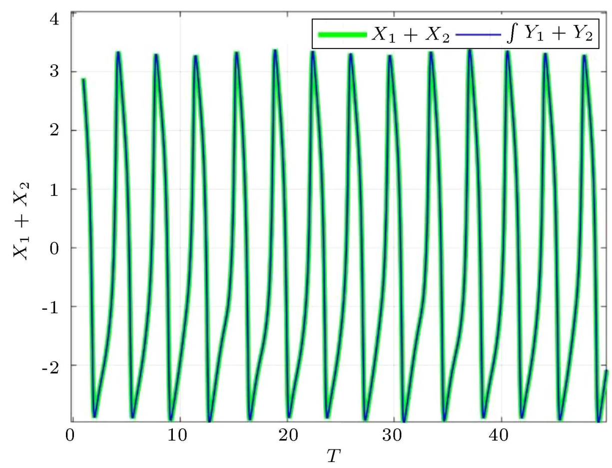

Figure 10. Integral of the summation of y variables in blue and the generation of the x variables summation in green.

its parameters are known, while the degree of the interaction (the coupling parameter) is unknown. The ultimate goal is to be able to calculate y_2 at any time by having abdominal recording. An attempt has been made to get some additional information that could bring us closer to the answer. For instance, the sum of x variables can also be obtained based on the model. Eq. (5) shows both x variables of the network:

$$\begin{cases} \dot{x}_1 = y_1 + \varepsilon(x_2 - x_1) \\ \dot{x}_2 = \left(\frac{1}{A}\right)(By_2) + \varepsilon(x_1 - x_2) = y_2 + \varepsilon(x_1 - x_2). \end{cases} \tag{5}$$

By summing the two sides of Eq. (5), it can be concluded that $y_1 + y_2 = \dot{x}_1 + \dot{x}_2$. Then, by integrating both sides, we have:

$$\int sum(y_1 + y_2) = \int \dot{x}_1 + \dot{x}_2 = sum(x_1 + x_2). \tag{6}$$

Therefore, recording the collective signal $y_1 + y_2$ with abdominal recording can end with the summation of x variables. Figure 10 shows the summation of variables calculated from the collective signal $y_1 + y_2$.

Considering Eulerian [77], the continuous form of Eq. (4) can be discretized as Eq. (7) shown in Box I. There are two ways to solve Eq. (7): step-by-step and high-order techniques. The step-by-step technique uses x and y summation signals at each moment and generates Eq. (8):

$$\begin{cases} x_1(i) + x_2(i) = sum(x_1 + x_2)(i) \\ y_1(i) + y_2(i) = sum(y_1 + y_2)(i) \end{cases} \quad i = 1, \ldots, N \tag{8}$$

Based on the summation signal, the relation can be written with a further step:

$$y_1(i+2) + y_2(i+2) = sum(y_1 + y_2)(i+2). \tag{9}$$

Since new unknowns are added to Eq. (9), the Euler relation is used to write the present step with the previous step variables:

$$y_1(i+2) + y_2(i+2) = y_1(i+1) + y_2(i+1)$$
$$+\Delta t\Big(-a(x_1(i+1) - w_1)(x_1(i+1) + w_2)y_1(i+1)$$
$$-x_1^3(i+1) + b\cos(ct)\Big) + \Delta t\left(\left(\frac{1}{B}\right)\right.$$
$$\Big(-a(Ax_2(i+1) - w_1)(Ax_2(i+1) + w_2)y_2(i+1)$$

$$\begin{cases} x_1(i+1) = x_1(i) + \Delta t\left(y_1(i) + \varepsilon(x_2(i) - x_1(i))\right) \\ y_1(i+1) = y_1(i) + \Delta t\left(-a(x_1(i) - w_1)(x_1(i) + w_2)y_1(i) - x_1^3(i) + b\cos(ct)\right) \\ x_2(i+1) = x_2(i) + \Delta t\left(\left(\frac{1}{A}\right)(By_2(i)) + \varepsilon\left(x_1(i) - x_2(i)\right)\right) \\ y_2(i+1) = y_2(i) + \Delta t\left(\left(\frac{1}{B}\right)\left(-a(Ax_2(i) - w_1)(Ax_2(i) + w_2)y_2(i) - \left(Ax_2(i)\right)^3 + b\cos(ct)\right)\right) \end{cases}$$

$$i = 1, ..., N-1. \tag{7}$$

Box I

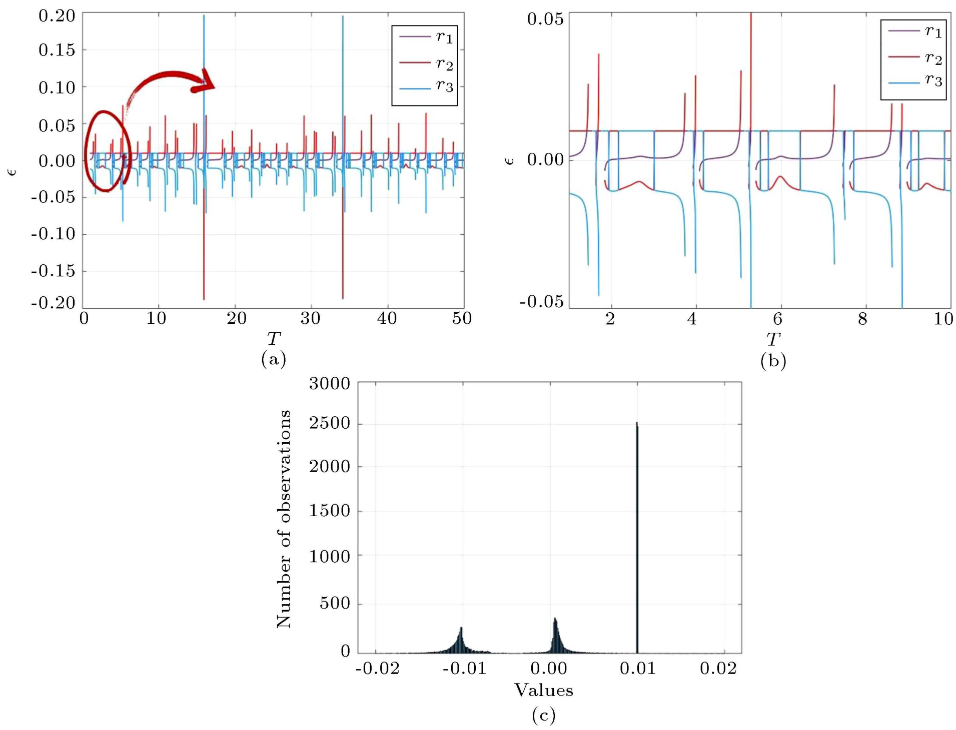

Figure 11. (a) Computed unknown coupling parameter, ε, in the time domain. (b) A zoomed plot of part a in the specified region. (c) Histogram of different answers for all the times.

$$-(Ax_2(i+1))^3 + b\cos(ct)\Big)\Big)$$

$$= sum(y_1 + y_2)(i+2). \qquad (10)$$

Of note, five equations are obtained: two equations from the x variables summation, two equations from the y variables summation (Eqs. (8) and (10)).

$$\begin{cases} x_1(i) + x_2(i) = sum(x_1 + x_2)(i) \\ y_1(i) + y_2(i) = sum(y_1 + y_2)(i) \\ x_1(i+1) + x_2(i+1) = sum(x_1 + x_2)(i+1) \\ y_1(i+1) + y_2(i+1) = sum(y_1 + y_2)(i+1) \\ Eq.10 \end{cases}$$

In addition, four equations have been achieved from the Euler discretization in Eq. (7). Finally, the problem leads to a system of nine equations and nine variables. Figure 11 shows the results for a part of the signal in the time domain.

As shown in Figure 11, this system of equations has three roots for coupling parameter, ε. Roots with imaginary values are omitted because they were not acceptable. One of the roots was equal to the value of 0.01 in all cases that remained visible on a continuous line at the mentioned value. In the histogram plot in Figure 11(c), the maximum intensity is the exact value of 0.01. Similarly, for other unknown values, $y_1(t)$ and $y_2(t)$, three roots can be calculated, while roots with imaginary values must be eliminated. Assume that M_1, M_2, and M_3 are three roots of y_1, and F_1, F_2, and F_3 are roots of y_2, in which only one answer is correct at a time. Figure 12 shows these roots.

Figure 13 illustrates the estimated variations in the maternal and fetal heart rates based on the calculated roots of y_1 (maternal heart) and y_2 (fetal heart) at any given time when the coupling coefficient is set to $\varepsilon = 0.01$.

The second approach involves an overview of the problem. By taking an overall look at the whole system of equations from the beginning to the end, it can be seen that our problem is broken into solving nine equations with nine unknown variables. However, there are solution methods with high-order equations, too. Meanwhile, in the previous method, variables in the next step are calculated once here and then again in the next. If all Euler's equations (Eq. (7)) are put together, as the equations are based on one step ahead, the problem is resolved upon solving the $4(N-1)$ equations and $4N+1$ variables. However, with the summation of x and y signals in Eq. (8), we have $2N$ equations as follows:

$$\begin{cases} x_1(1) + x_2(1) = sum(x_1 + x_2)(1) \\ y_1(1) + y_2(1) = sum(y_1 + y_2)(1) \\ \vdots \\ x_1(N) + x_2(N) = sum(x_1 + x_2)(N) \\ y_1(N) + y_2(N) = sum(y_1 + y_2)(N) \end{cases}$$

In conclusion, by assuming the signal length N, there

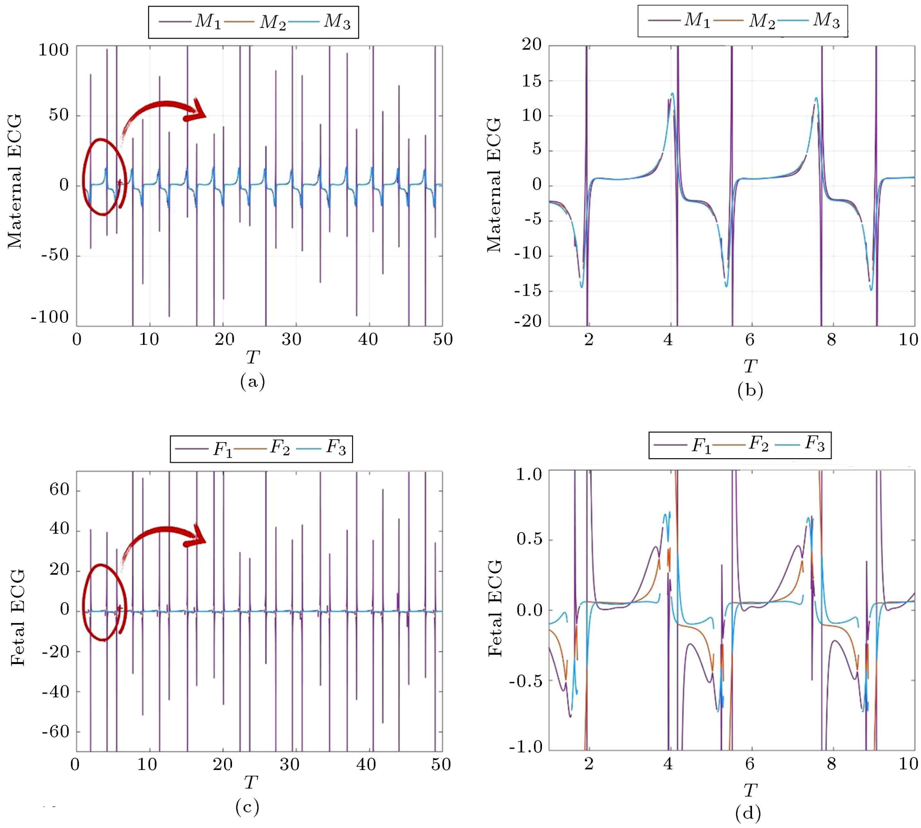

Figure 12. Separation of mother and fetus hearts by computed unknowns: (a) M_1, M_2, and M_3 as three roots in computing y_1, (b) a zoomed plot of it in the specified region, (c) F_1, F_2, and F_3 as three roots in computing y_2, and (d) a zoomed plot of it in the specified region.

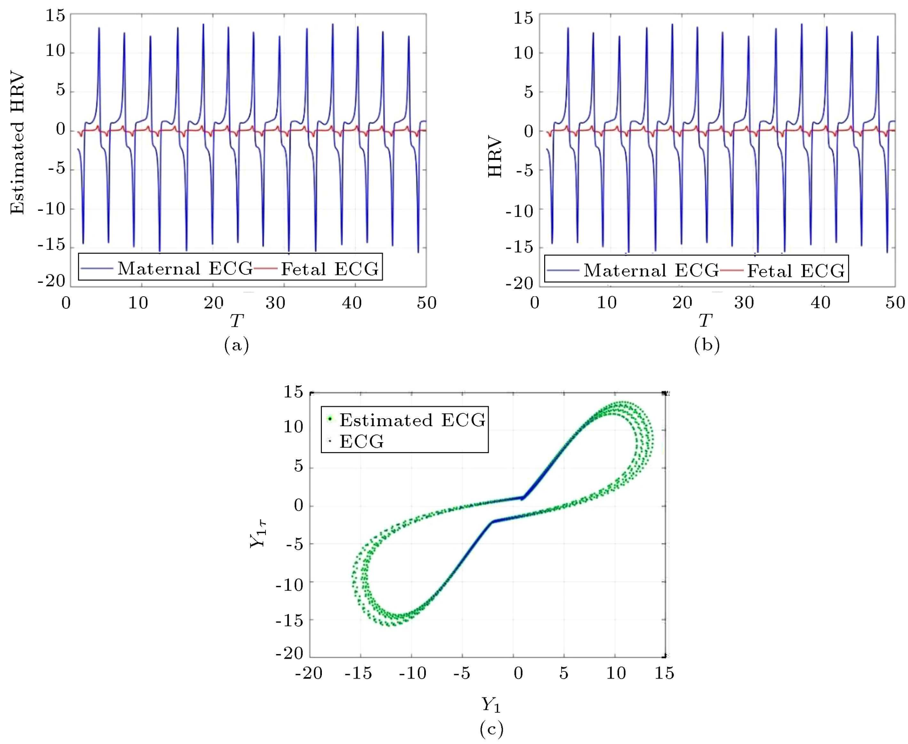

Figure 13. (a) Estimated maternal and fetal HRV. (b) Actual maternal and fetal HRV. (c) Phase space of estimated maternal ECG in green and natural maternal ECG in blue.

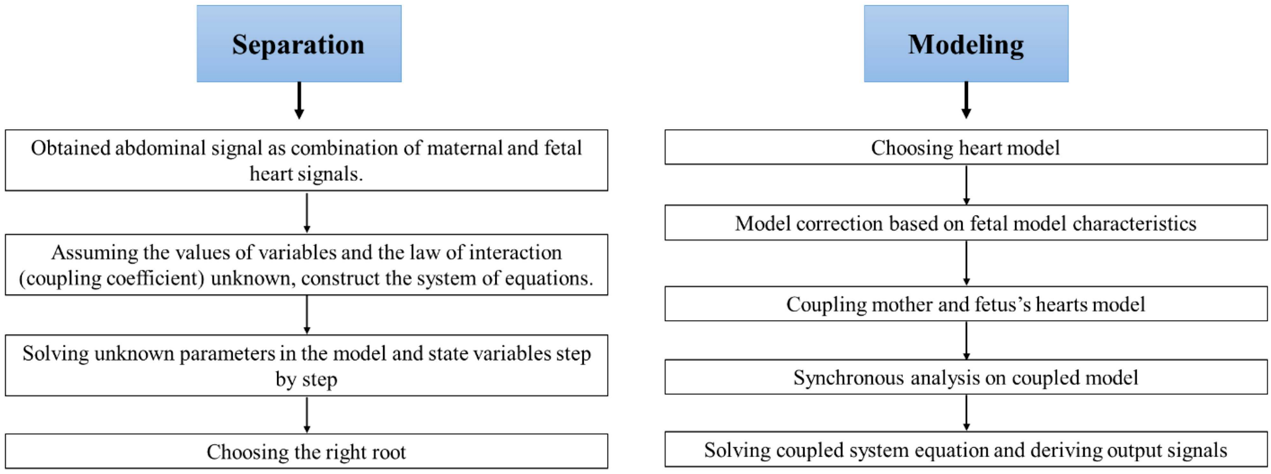

Figure 14. Block diagram of the proposed algorithm that summarizes the method at two phases. At the modeling phase, a non-identical network of maternal and fetal hearts is synchronized. The separation phase summarizes how abdominal signal breaks down into maternal and fetal heart signals.

are $4(N-1)$ Eulerian system equations and summation equations (Eq. (8)) with $4N+1$ variables (x, y, and the coupling coefficient). Therefore, the number of equations is $6N-4$, while the number of unknowns is $4N+1$.

Generally, it can be concluded that for any basic m-dimensional model, especially the heart model with nonlinear interaction function and a signal with length N, there are $N+2m(N-1)$ equations with $2mN+1$ variables. The $2m(N-1)$ equations are captured from Eulerian system equations, and N comes from the summation relations. The $2mN$ variables are the state variables in each step with one coupling coefficient.

Moreover, the model parameters can be considered as unknown variables. In this problem, the number of equations is $N+2m(N-1)$ and the number of variables turns to $2mN+A$ (A is the number of the model parameters).

5. Discussion

This paper is basically constructed of two modeling and separation phases. At the first phase, a heart model was presented. The selected model functions based on modification of the Duffing-Van der Pol system, which is entirely optional. To develop this method, any other model can be replaced with Van der Pol, as long as the model is compatible with the model chaotic dynamics of the heart system. In order to analyze the chaotic dynamics of the system, the bifurcation and Lyapunov exponents diagrams were plotted. One of the considerable challenges on fECG separation was the distinction between maternal and fetal ECG amplitudes caused by structural differences in the fetal heart. Therefore, the fetal heart model was obtained by creating coefficients in the heart model. These coefficients can be modified as desired in Section 2.2. In the worst case scenario, fECG amplitude was chosen 20 times weaker than mECG amplitude. Choosing another value out of the boundary to illustrate the strength of mECG can reproduce the whole computation as well. In other words, the selected value depends on the expected ratio of maternal to fetal amplitudes. Besides, the non-identical coupling of the maternal and fetal hearts showed the interaction between maternal and fetal hearts. The coupling was assumed linear in the x variables equations. The effect of CP on each other was studied. Finally, the synchronization pattern of this network was checked.

At the separation phase, the values of variables and the law of interaction (coupling coefficient) were assumed to be unknown. The system of equations according to the interactive network equation and the abdominal signal was constructed. Two methods for performing calculations were discussed: a step-by-step method and high-order equations. In the step-by-step method, while solving the equation at the ith iteration, additional variables were computed (variables in the next step were calculated one time in the present step and once again in the next). This study proposed a high-order equation to reduce computational complexity by reducing additional unknowns in another approach. Solving equations is done only for the step-by-step method, but an analytical explanation for higher-order equations has been proposed. In the study of the high-order equation, more parameters, in addition to the interaction coefficient, can be assumed unknown. In the end, the fetal heart signal can be separated by selecting the correct roots. The diagram in Figure 14 summarizes the procedure application.

6. Conclusion

This work presented the modified Van der Pol model to separate the fetal Electrocardiagrams (fECGs) based on the abdominal recordings. To this end, two phases were employed: modeling and separation phases. At the modeling phase, a heart model was proposed based on a modified Duffing-Van der Pol oscillator. Because of the fetal heart's structural changes, some parameters were added to the model; thus, the model can illustrate the fetal cardiac state faultlessly. During pregnancy, the hearts of the mother and fetus interacted with each other; hence, the two heart models were coupled linearly. Based on the pattern synchronization, the coupling parameter was calculated. At the separation phase, the obtained combination of maternal and fetal heart signals was considered as the abdominal ECG (aECG). Then, the system of equations with the problem assumptions was constructed by solving the system of equations and calculating the variables, i.e., maternal and fetal signals. Finally, the state variables were calculated in each step, making it possible to separate the maternal signal from the fetal one.

References

1. Warnes, C.A., Liberthson, R., Danielson, G.K., et al. "Task force 1: the changing profile of congenital heart disease in adult life", *J. Am. Coll. Cardiol.*, **37**(5), pp. 1170–1175 (2001).
2. Neilson, J.P. "Fetal electrocardiogram (ECG) for fetal monitoring during labour", *Cochrane Database Syst. Rev.*, **2015**(12), CD000116 (2015).
3. Westgate, J., Harris, M., Curnow, J.S., et al. "Plymouth randomized trial of cardiotocogram only versus ST waveform plus cardiotocogram for intrapartum monitoring in 2400 cases", *Am. J. Obstet. Gynecol.*, **169**(5), pp. 1151–1160 (1993).
4. Newbold, S., Wheeler, T., and Clewlow, F. "Comparison of the T/QRS ratio of the fetal electrocardiogram and the fetal heart rate during labour and the relation of these variables to condition at delivery", *BJOG*, **98**(2), pp. 173–178 (1991).
5. Jaros, R., Martinek, R., and Kahankova, R. "Non-adaptive methods for fetal ECG signal processing: A review and appraisal", *Sensors*, **18**(11), 3648 (2018).
6. Sameni, R. and Clifford, G.D. "A review of fetal ECG signal processing; issues and promising directions", *Open Pacing Electrophysiol. Ther. J.*, **3**, pp. 4–20 (2010).
7. Alnuaimi, S.A., Jimaa, S., and Khandoker, A.H. "Fetal cardiac doppler signal processing techniques: challenges and future research directions", *Front. Bioeng. Biotechnol.*, **5**, p. 82 (2017).
8. Martinek, R., Kahankova, R., Jezewski, J., et al. "Comparative effectiveness of ICA and PCA in extraction of fetal ECG from abdominal signals: Toward non-invasive fetal monitoring", *Front. Physiol.*, **9**, p. 648 (2018).
9. Clifford, G.D., Silva, I., Behar, J., et al. "Non-invasive fetal ECG analysis", *Physiol. Meas.*, **35**(8), p. 1521 (2014).
10. Behar, J., Oster, J., and Clifford, G.D. "Non-invasive FECG extraction from a set of abdominal sensors", In *2013 Computing in Cardiology Conference (CinC 2013)* (No. ISBN 9781479908851), pp. 297–300, Institute of Electrical and Electronics Engineers (IEEE), Curran Associates, Inc (2013).
11. Li, S., Hou, Z., and Li, Q. "A new algorithm for extracting fetal ECG signal using singular value decomposition method", In *Acoustics, Speech, and Signal Processing, ICASSP-92., 1992 IEEE International Conference on*, pp. 585–588 (1992).
12. Queyam, A.B., Pahuja, S.K., and Singh, D. "Non-invasive feto-maternal well-being monitoring: A review of methods", *J. Eng. Sci. Technol. Rev.*, **10**(1), pp. 177–190 (2017).
13. Zarzoso, V., Millet-Roig, J., and Nandi, A. "Fetal ECG extraction from maternal skin electrodes using blind source separation and adaptive noise cancellation techniques", in *Computers in Cardiology 2000*, 2000, pp. 431–434.
14. Zhou, X., Engler, P., and Coblentz, M.G. "Adaptive filter application in fetal electrocardiography", in *Computer-Based Medical Systems, 1992. Proceedings., Fifth Annual IEEE Symposium on,* pp. 656–662 (1992).
15. Kam, A. and Cohen, A. "Detection of fetal ECG with IIR adaptive filtering and genetic algorithms", in *Acoustics, Speech, and Signal Processing, Proceedings., IEEE International Conference on*, pp. 2335–2338 (1999).
16. Horner, S., Holls, W., and Crilly, P.B. "Non-invasive fetal electrocardiograph enhancement", in *Computers in Cardiology Proceedings of*, 1992, pp. 163–166 (1992).
17. Kanjilal, P.P., Palit, S., and Saha, G. "Fetal ECG extraction from single-channel maternal ECG using singular value decomposition", *IEEE. Trans. Biomed. Eng.*, **44**(1), pp. 51–59 (1997).
18. Vigneron, V., Paraschiv-Ionescu, A., Azancot, A., et al. "Fetal electrocardiogram extraction based on non-stationary ICA and wavelet denoising", in *Signal Processing and Its Applications, 2003. Proceedings. Seventh International Symposium on*, pp. 69–72 (2003).
19. Lee, J., Park, K., and Lee, K. "Temporally constrained ICA-based foetal ECG separation", *Electron. Lett.*, **41**(21), pp. 1158–1160 (2005).
20. Gao, P., Chang, E.-C., and Wyse, L. "Blind separation of fetal ECG from single mixture using SVD and ICA", in *Information, Communications and Signal Processing, 2003 and Fourth Pacific Rim Conference on Multimedia. Proceedings of the 2003 Joint Conference of the Fourth International Conference on*, pp. 1418–1422 (2003).
21. Bell, A.J. and Sejnowski, T.J. "The 'independent components' of natural scenes are edge filters", *Vis. Res.*, **37**(23), pp. 3327–3338 (1997).

22. Datian, Y. and Xuemei, O. "Application of wavelet analysis in detection of fetal ECG", in *Engineering in Medicine and Biology Society, 1996. Bridging Disciplines for Biomedicine. Proceedings of the 18th Annual International Conference of the IEEE*, pp. 1043–1044 (1996).

23. Khamene, A. and Negahdaripour, S. "A new method for the extraction of fetal ECG from the composite abdominal signal", *IEEE. Trans. Biomed. Eng.*, **47**(4), pp. 507–516 (2000).

24. Vaidya, R.R. and Chaitra, N. "Comparison of Adaptive filters in extraction of Fetal ECG", in *2020 International Conference on Smart Electronics and Communication (ICOSEC)*, pp. 1066–1070 (2020).

25. Kahankova, R., Martinek, R., and Bilik, P. "Fetal ECG extraction from abdominal ECG using RLS based adaptive algorithms", in *2017 18th International Carpathian Control Conference (ICCC)*, pp. 337–342 (2017).

26. Nasiri, M. "Fetal electrocardiogram signal extraction by ANFIS trained with PSO method", *Int. J. Electr. Comput. Eng.*, **2**(2), p. 247 (2012).

27. Uddin, Z., Orakzai, F., and Qamar, A. "Order and phase ambiguities correction in the ICA based separation of speech signals", *Int. J. Speech Technol.*, **23**(2), pp. 459–469 (2020).

28. Jiménez-González, A. and Castañeda-Villa, N. "Blind extraction of fetal and maternal components from the abdominal electrocardiogram: An ICA implementation for low-dimensional recordings", *Biomed. Signal Process. Control.*, **58**, 101836 (2020).

29. Baldazzi, G., Sulas, E., Brungiu, E., et al. "Wavelet-based post-processing methods for the enhancement of non-invasive fetal ECG", in *2019 Computing in Cardiology (CinC)*, pp. 1–4 (2019).

30. Vijila, C.K.S., Kanagasabapathy, P., Johnson, S., et al. "Interference cancellation in FECG using artificial intelligence techniques", in *Intelligent Sensing and Information Processing, ICISIP 2006. Fourth International Conference on*, pp. 174–177 (2006).

31. Ungureanu, M., Bergmans, J.W., Mischi, M., et al. "Improved method for fetal heart rate monitoring", in *Engineering in Medicine and Biology Society, 2005. IEEE-EMBS 2005. 27th Annual International Conference of the*, pp. 5916–5919 (2006).

32. Yang, Y. and Guo, C. "Blind extraction for noisy fetal electrocardiogram by using Gaussian m oments", in *Fourth International Conference on Natural Computation*, pp. 44–47 (2008).

33. Zhang, Z.-L. and Yi, Z. "Variable step-size extraction algorithm for extracting fetal electrocardiogram", in *Neural Networks and Brain, 2005. ICNN&B'05. International Conference on*, pp. 434–437 (2005).

34. Egan, F. "Computational models: A modest role for content", *Stud. Hist. Philos. Sci. A*, **41**(3), pp. 253–259 (2010).

35. An, G., Mi, Q., Dutta-Moscato, J., et al. "Agent-based models in translational systems biology", *Wiley Interdiscip. Rev. Syst. Biol. Med.*, **1**(2), pp. 159–171 (2009).

36. Barlas, Y. "Formal aspects of model validity and validation in system dynamics", *Syst. Dyn. Rev.*, **12**(3), pp. 183–210 (1996).

37. Kresh, J.Y., Izrailtyan, I., and Wechsler, A.S. "The heart as a complex adaptive system", in *Unifying Themes in Complex Systems*, Ed: CRC Press, pp. 289–304 (2018).

38. Lim, G.B. "Evolutionary adaptations of human hearts", *Nat. Rev. Cardiol.*, **16**(12), pp. 700–700 (2019).

39. Bonabeau, E. "Agent-based modeling: Methods and techniques for simulating human systems", *Proceedings of the National Academy of Sciences*, **99**(suppl 3), pp. 7280–7287 (2002).

40. Jovanovic, V.T. and Kazerounian, K. "Using chaos to obtain global solutions in computational kinematics", *Transactions-American Society of Mechanical Engineers Journal of Mechanical Design*, **120**(2), pp. 299–304 (1998).

41. Eskov, V., Eskov, V., Vochmina, J., et al. "The evolution of the chaotic dynamics of collective modes as a method for the behavioral description of living systems", *Mosc. Univ. Phys. Bull.*, **71**(2), pp. 143–154 (2016).

42. Bazeia, D., Pereira, M., Brito, A., et al. "A novel procedure for the identification of chaos in complex biological systems", *Sci. Rep.*, **7**(1), pp. 1–9 (2017).

43. Harrar, K. and Hamami, L. "The box counting method for evaluate the fractal Dimension in radiographic images", in *6th WSEAS International Conference on Circuits, Systems, Electronics, Control & Signal Processing*, Egypt, p. 385 (2007).

44. Mishra, A.K. and Raghav, S. "Local fractal dimension based ECG arrhythmia classification", *Biomed. Signal Process. Control.*, **5**(2), pp. 114–123 (2010).

45. Sharma, V. "Deterministic chaos and fractal complexity in the dynamics of cardiovascular behavior: perspectives on a new frontier", *Open Cardiovasc. Med. J.*, **3**, p. 110 (2009).

46. Wagner, C.D. and Persson, P.B. "Chaos in the cardiovascular system: an update", *Cardiovasc. Res.*, **40**(2), pp. 257–264 (1998).

47. Chialvo, D.R., Michaels, D.C., and Jalife, J. "Supernormal excitability as a mechanism of chaotic dynamics of activation in cardiac Purkinje fibers", *Circ. Res.*, **66**(2), pp. 525–545 (1990).

48. Qu, Z., Hu, G., Garfinkel, A., et al. "Nonlinear and stochastic dynamics in the heart", *Phys. Rep.*, **543**(2), pp. 61–162 (2014).

49. Van Der Pol, B. and Van Der Mark, J. "LXXII. The heartbeat considered as a relaxation oscillation, and an electrical model of the heart", *Lond. Edinb. Dubl. Phil. Mag. J. Sci.*, **6**(38), pp. 763–775 (1928).

50. Grudziński, K. and Żebrowski, J.J. "Modeling cardiac pacemakers with relaxation oscillators", *Physica A*, **336**(1–2), pp. 153–162 (2004).

51. Zduniak, B., Bodnar, M., and Foryś, U. "A modified van der Pol equation with delay in a description of the heart action", *Int. J. Appl. Math. Comput. Sci.*, **24**(4), pp. 853–863 (2014).

52. Raja, M.A.Z., Shah, F.H., and Syam, M.I. "Intelligent computing approach to solve the nonlinear Van der Pol system for heartbeat model", *Neural. Comput. Appl.*, **30**(12), pp. 3651–3675 (2018).

53. dos Santos, A.M., Lopes, S.R., and Viana, R.R.L. "Rhythm synchronization and chaotic modulation of coupled Van der Pol oscillators in a model for the heartbeat", *Physica A*, **338**(3–4), pp. 335–355 (2004).

54. Pereira, T.L., de Paula, A.S., Cheffer, A., et al. "Bifurcation from normal functioning to pathologies in a cardiac model using a three modified coupled van der pol Oscillator", in *Proceedings of the XVIII International Symposium on Dynamic Problems of Mechanics (DINAME 2019)*, Brazil (2019).

55. Gois, S.R. and Savi, M.A. "An analysis of heart rhythm dynamics using a three-coupled oscillator model", *Chaos Solitons Fractals*, **41**(5), pp. 2553–2565 (2009).

56. Boccaletti, S., Hwang, D.-U., Chavez, M., et al. "Synchronization in dynamical networks: Evolution along commutative graphs", *Phys. Rev. E*, **74**(1), 016102 (2006).

57. Hindes, J. and Schwartz, I.B. "Rare slips in fluctuating synchronized oscillator networks", *Chaos*, **28**(7), 071106 (2018).

58. Pikovsky, A. and Rosenblum, M. "Dynamics of globally coupled oscillators: Progress and perspectives", *Chaos: An Interdisciplinary Journal of Nonlinear Science*, **25**(9), 097616 (2015).

59. Zhang, Y., Nishikawa, T., and Motter, A.E. "Asymmetry-induced synchronization in oscillator networks", *Phys. Rev. E,* **95**(6), 062215 (2017).

60. Zhang, L., Motter, A.E., and Nishikawa, T. "Incoherence-mediated remote synchronization", *Phys. Rev. Lett.*, **118**(17), 174102 (2017).

61. Chen, T., Peng, S., and Zhang, Z. "Finite-time synchronization of Markovian jumping complex networks with non-identical nodes and impulsive effects", *Entropy*, **21**(8), p. 779 (2019).

62. Panahi, S. and Jafari, S. "New synchronization index of non-identical networks", *Discrete Contin. Dyn. Syst. Ser. S*, **14**(4), p. 1359 (2021).

63. Silvestri, F., Acciarito, S., and Khanal, G.M. "Relationship between mathematical parameters of modified Van der Pol Oscillator model and ECG morphological features", *Int. J. Adv. Sci. Eng. Inf. Technol.*, **9**(2), pp. 601–608 (2019).

64. Rajagopal, K., Li, C., Nazarimehr, F., et al. "Chaotic dynamics of modified wien bridge oscillator with fractional order memristor", *Radioengineering*, **28**(1), pp. 165–174 (2019).

65. Kim, Y.J., Park, C.S., and Kim, K.W. "Chaos time series model for nonlinear multi-step ahead prediction", in *Proceedings of BS2015:14th Conference of International Building Performance Simulation Association*, Hyderabad, India (2015).

66. Fathima, T. and Jothiprakash, V. "Behavioural analysis of a time series-A chaotic approach", *Sadhana*, **39**(3), pp. 659–676 (2014).

67. Hajiloo, R., Salarieh, H., and Alasty, A. "Chaos control in delayed phase space constructed by the Takens embedding theory", *Commun. Nonlinear. Sci. Numer. Simul.*, **54**, pp. 453–465 (2018).

68. Xu, P. "Differential phase space reconstructed for chaotic time series", *Appl. Math. Model.*, **33**(2), pp. 999–1013 (2009).

69. Pikovsky, A., Rosenblum, M., and Kurths, J. "Synchronization: a universal concept in nonlinear sciences", 12: Cambridge University Press (2003).

70. Ávila, G.R., Kurths, J., Guisset, J.-L., et al. "How do small differences in nonidentical pulse-coupled oscillators induce great changes in their synchronous behavior?", *Eur. Phys. J. : Spec. Top.*, **223**(13), pp. 2759–2773 (2014).

71. Xiang, J. and Chen, G. "On the V-stability of complex dynamical networks", *Automatica*, **43**(6), pp. 1049–1057 (2007).

72. Hill, D.J. and Zhao, J. "Global synchronization of complex dynamical networks with non-identical nodes", in *2008 47th IEEE Conference on Decision and Control,* pp. 817–822 (2008).

73. Zhao, J., Hill, D.J., and Liu, T. "Passivity-based output synchronization of dynamical networks with non-identical nodes", in *49th IEEE Conference on Decision and Control (CDC)*, pp. 7351–7356 (2010).

74. Zhang, Y. and Motter, A.E. "Identical synchronization of nonidentical oscillators: when only birds of different feathers flock together", *Nonlinearity*, **31**(1) (2017).

75. Rosenblum, M.G., Pikovsky, A.S., and Kurths, J. "Phase synchronization of chaotic oscillators", *Phys. Rev. Lett.*, **76**(11), 1804 (1996).

76. Wen, D., Zhou, Y., and Li, X. "A critical review: coupling and synchronization analysis methods of EEG signal with mild cognitive impairment", *Front. Aging Neurosci.*, **7**, p. 54 (2015).

77. Zandi-Mehran, N., Jafari, S., and Golpayegani, S.M.R.H. "Signal separation in an aggregation of chaotic signals", *Chaos Solitons Fractals*, **138**, 109851 (2020).

Biographies

Nazanin Zandi Mehran was born in 1989 in Tehran. She received her BSc degree in Biomedical Engineering and Applied Mathematics in 2012 and her MSc degree in Biomedical Engineering in 2014 from Amirkabir University of Technology, Tehran, Iran. Currently, she is a PhD student at the Amirkabir University of Technology. Her main research interest includes chaos theory.

Seyyed Mohammad Reza Hashemi Golpayegani is a Professor at the Biomedical Engineering Department of Amirkabir University of Technology, Tehran, Iran and was the Minister of Culture and Higher Education in Iran from 1983 to 1987. He has authored and co-authored numerous papers in Electrical and Biomedical Engineering and has also been active in the field of Philosophy of Science and Engineering Education. He is credited with the publication of a number of articles in international scientific journals in the fields mentioned.